X-Ray Diffuse Scattering due to Polarons in a Colossal Magnetoresistive Manganite

S. Shimomura,[1] N. Wakabayashi,[1] H. Kuwahara,[2,*] and Y. Tokura[2,3]
[1]*Department of Physics, Faculty of Science and Technology, Keio University, 3-14-1 Hiyoshi, Kohoku-ku, Yokohama 223-8522, Japan*
[2]*Joint Research Center for Atom Technology (JRCAT), Tsukuba 305-8562, Japan*
[3]*Department of Applied Physics, University of Tokyo, Tokyo 113-8656, Japan*
(Received 14 July 1999)

X-ray scattering study on $(Nd_{0.125}Sm_{0.875})_{0.52}Sr_{0.48}MnO_3$ has revealed the existence of diffuse scattering in the paramagnetic phase. Its intensity increases with decreasing temperature, but it vanishes at the ferromagnetic transition temperature. This result indicates that local lattice distortion arises from the localization of electrons on Mn sites (polarons). The intensity distributions are in agreement with calculations based on polarons associated with the Jahn-Teller distortion. Correlation between the distortion fields seems to be related to the formation of charge ordering.

PACS numbers: 75.30.Vn, 63.20.Kr, 71.30.+h, 71.38.+i

Manganese oxide compounds with distorted perovskite structures, $A_{1-x}B_xMnO_3$ (A = trivalent rare earth ion, B = divalent alkali earth ion), have received great interests because of their colossal magnetoresistance (CMR). Attempts have been made to interpret the coexistence of the ferromagnetic state and the metallic state in terms of the double-exchange mechanism [1]. However, neither the large resistivity observed above the ferromagnetic transition temperature (T_C) nor the CMR can be explained by the double-exchange mechanism alone [2]. A plausible supplemental mechanism has been suggested to be strong electron-lattice coupling due to the Jahn-Teller (JT) effect of Mn^{3+} [3,4]. The localization of carriers (e_g state) on Mn sites produces lattice polarons in the paramagnetic insulating phase, and the hopping of the electrons dressed with the lattice distortion plays an essential role in the transport properties. Below T_C, the ferromagnetic metallic phase becomes stable, and the lattice distortion spreads out in the large spatial region. The existence of the local lattice distortion due to polarons has been experimentally suggested by x-ray absorption fine structure [5], pair-density functions determined by neutron diffraction [6], and optical experiments [7–9]. However, the displacement patterns of the local lattice distortion obtained by these measurements do not agree with each other. A probable pattern of the lattice distortion is that of the JT distortion of $Mn^{3+}O_6$ octahedra. The correlation between polarons becomes significant when their concentration is large. It is considered to be important in determining the transport property as well as in the ordering of Mn^{3+} and Mn^{4+} ions accompanied by the cooperative JT transition.

The $(Nd_{1-y}Sm_y)_{0.5}Sr_{0.5}MnO_3$ crystals are good systems to study for clarifying the relationship between the transport property, on one hand, and the formation of polarons and their correlation, on the other. The average ionic radius of the A site, which depends on y, changes the transport properties systematically [10]. The crystal with $y = 0$ shows a charge-ordering antiferromagnetic transition and no significant change in the resistivity at T_C. As y increases, the transition temperature T_C becomes lower and a large decrease in the resistivity at T_C becomes more prominent. In the crystals with $0.85 \leq y \leq 0.95$, the charge-ordered phase disappears and the resistivity shows the large drop at T_C. Furthermore, the lattice parameters change discontinuously at T_C and the inverse magnetization deviates from the Curie-Weiss behavior above T_C. These systematic changes for varying y suggest that the competition between the charge-ordering antiferromagnetic interaction and the double-exchange ferromagnetic interaction causes the enhancement of the resistivity above T_C associated with the charge-ordering instability. The purpose of the present x-ray scattering study is to clarify the relationship between the insulator-metal transition concomitant with the ferromagnetic transition and the local lattice distortion due to the localization of carriers on Mn sites.

Single crystals of $(Nd_{0.125}Sm_{0.875})_{0.52}Sr_{0.48}MnO_3$ were grown by the floating zone method. The observed resistivity and the inverse magnetization are quite similar to those of the half-doped crystal $(Nd_{0.125}Sm_{0.875})_{0.5}Sr_{0.5}MnO_3$ reported previously [10]. X-ray scattering measurements were performed using a two-axis diffractometer with Mo-$K\alpha$ radiation (50 kV, 150 mA) monochromatized by the 002 reflection of a pyrolytic graphite crystal. In order to eliminate unwanted scattering, a pyrolytic graphite crystal was used as an analyzer crystal as well. Measurements were carried out using a closed-cycle refrigerator. The crystal structure is orthorhombic with a pseudocubic relation of the lattice parameters specified by $a \simeq b \simeq c/\sqrt{2} \simeq \sqrt{2}\,a_c$, where a_c is the lattice parameter of the cubic-perovskite lattice. As-grown crystals were composed of domains, and it was difficult to obtain single domain samples. Fundamental Bragg reflections from different domains, such as $(2n, 0, 0)$, $(0, 2n, 0)$, and $(n, n, 2n)$, were nearly indistinguishable. In this paper, all the reflections are indexed on the basis of one domain for the sake of convenience. Two samples were prepared in the form of plates with their surfaces parallel to either the (010) or (110) planes. The sample sizes were

 © 1999 The American Physical Society

approximately $2 \times 2 \times 0.3$ mm^3. The transition temperature T_C of 133 K was determined by magnetization, resistivity, and x-ray scattering measurements.

The temperature dependence of some of the scattering profiles along the [100] direction through the $(0, 10, 0)$ point is shown in Fig. 1. The profiles contain the sharp fundamental Bragg peaks (only the tail portion in the figure) and the diffuse scattering components. The diffuse intensity increases as T_C is approached from room temperature, but it falls sharply below T_C. The profiles near T_C seem to have humps around $(\pm 0.30, 10, 0)$. Figure 2(a) shows the temperature dependence of the intensity at $(-0.30, 10, 0)$. This temperature dependence is very similar to the rapid increase and drop in the resistivity as shown in Fig. 2(b). This close relationship strongly suggests that the diffuse scattering arises from the local lattice distortion produced by the localization of the carriers on Mn sites. The increase in the diffuse intensity may be due to the lower hopping rate of the e_g electrons, a longer lifetime of polarons, resulting in the larger distortion field. This may also be regarded as the increase in the effective number of polarons. The abrupt disappearance of its intensity below T_C indicates that the local lattice distortion vanishes due to complete delocalization of the e_g electrons.

In order to determine the pattern of the distortion field produced by polarons, we measured the intensity distributions of the diffuse scattering in the $[hk0]$ reciprocal lattice plane [11]. The contour plots of the diffuse scattering observed at 136 K around the $(0, 10, 0)$, $(4, 10, 0)$, and $(6, 6, 0)$ Bragg peaks are shown in Figs. 3(a), 3(b), and 3(c), respectively. The diffuse intensity distributions show characteristic patterns depending on the reciprocal lattice points. Those around the $(0, 10, 0)$ and $(4, 10, 0)$ reflections extend along the [100] direction. A butterfly-shaped pattern extending along the [100] and [010] is seen around $(6, 6, 0)$. The streaks passing through the reciprocal lattice points and extending toward the origin of the reciprocal lattice are due to contamination by radiation having wavelengths slightly different from that of the $K\alpha$ radiation. There are Bragg peaks from different domains centered around $(0.1, 10, 0)$ in Fig. 3(a) and $(4.1, 10, 0)$ in Fig. 3(b). The small peaks around $(h \pm 0.5, k \pm 0.5, 0)$ and $(h \pm 0.5, k \mp 0.5, 0)$ also arise from domain structures. For example, the one centered around $(0.5, 10.5, 0)$ corresponds to $(5, 5, 11)$ of a different domain.

The characteristic distributions of the diffuse intensity can be interpreted as a scattering due to polarons associated with the JT effect. The localization of an e_g electron on a Mn site, Mn^{3+}, is assumed to cause elongation of two Mn-O bonds and contractions of four Mn-O bonds in the $Mn^{3+}O_6$ octahedron as shown in Fig. 4. The atomic displacements induce a distortion field in the surrounding lattice. The scattering intensity due to the polaron can be calculated in the same manner as calculating the Huang scattering intensity for the lattice distortion [12,13]. We assume that the polarons are randomly distributed and those strain fields are independent of each other for the simplicity of the calculation. The dipole force tensor was chosen to have symmetries corresponding to the distortion of the $Mn^{3+}O_6$ octahedra. The elastic constants have not been reported for the present compound, and we used $c_{11} = 206$, $c_{12} = 111$, and $c_{44} = 60.2$ GPa reported for $La_{0.83}Sr_{0.17}MnO_3$ at 200 K [14]. The total intensity is

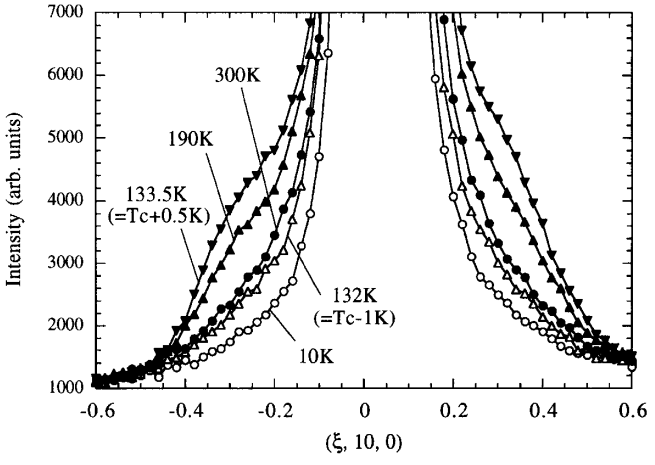

FIG. 1. Temperature dependence of some of the scattering profiles along the [100] direction through the $(0, 10, 0)$ point. With decreasing temperature from 300 K, the diffuse intensity increases but abruptly vanishes at the ferromagnetic transition temperature ($T_C = 133$ K).

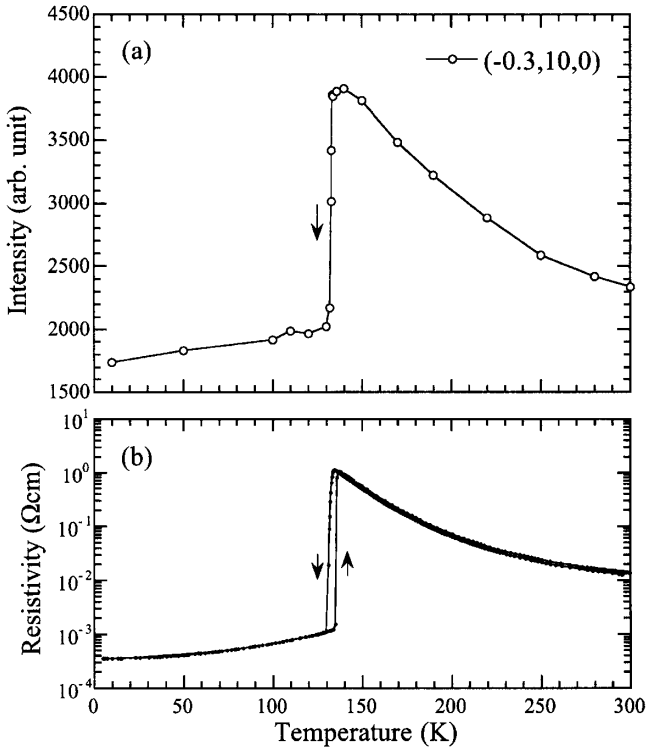

FIG. 2. Temperature dependence of (a) the diffuse scattering intensity at $(-0.30, 10, 0)$ and (b) the resistivity.

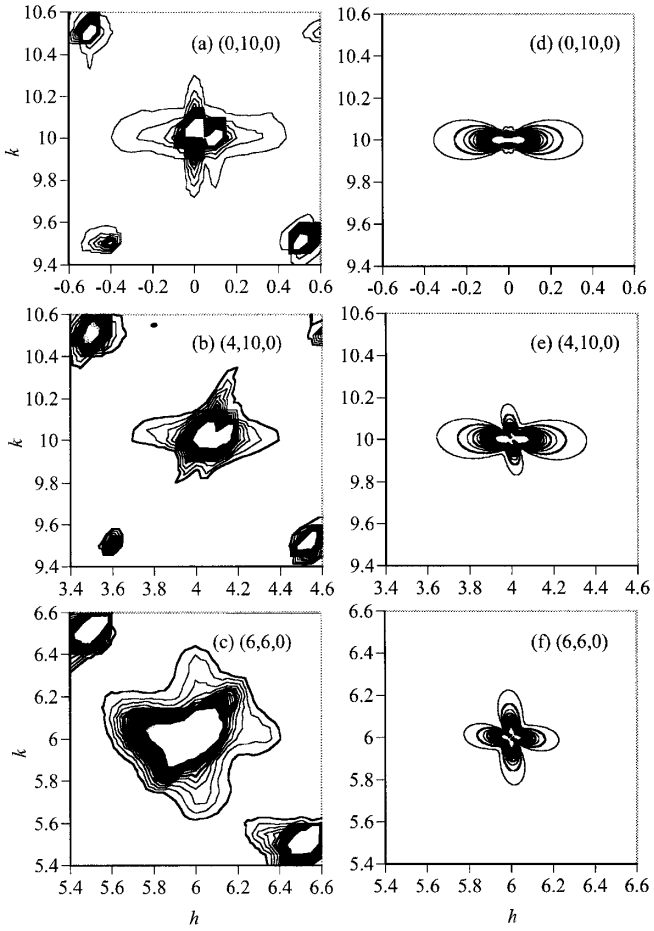

FIG. 3. Contour plots of the diffuse scattering intensities observed at 136 K around the (a) $(0, 10, 0)$, (b) $(4, 10, 0)$, and (c) $(6, 6, 0)$ Bragg peaks. The diffuse intensity distributions around $(0, 10, 0)$ and $(4, 10, 0)$ extend along the [010] direction. A butterfly-shaped pattern extending along [100] and [010] is seen around $(6, 6, 0)$. The streaks passing through the reciprocal lattice points and extending toward the origin of the reciprocal lattice are due to contamination by radiation having wavelengths slightly different from that of $K\alpha$ radiation. Calculated contour plots around the (d) $(0, 10, 0)$, (e) $(4, 10, 0)$, and (f) $(6, 6, 0)$ reflections.

obtained by superimposing the intensities calculated for the displacement patterns resulting from permuting x, y, and z coordinates. This superposition corresponds to the pseudocubic multidomain structure and randomly oriented polarons. The calculated intensities around the $(0, 10, 0)$, $(4, 10, 0)$, and $(6, 6, 0)$ peaks are shown in Figs. 3(d), 3(e), and 3(f), respectively. Although the small extrusions nearly along the [010] direction around the $(4, 10, 0)$ peak could not be detected on account of the contamination streak, overall agreement between the calculations and observations is satisfactory. Thus, the diffuse intensity should be attributed to polarons associated with the JT distortion.

As discussed later, correlation between polarons probably develops with decreasing temperature toward T_C and it seems to be related to the charge ordering. The charge ordering is accompanied by the ordering of two types of distorted $Mn^{3+}O_6$ octahedra: the one shown in Fig. 4 and the other with the x and y axes exchange. We also calculated the distributions of the diffuse intensities based on the existence of polarons associated with two such distortions. The calculated distributions are almost indistinguishable from those, shown in Fig. 3, obtained as a sum of the contributions resulting from permuting x, y, and z coordinates.

In an attempt to eliminate the contamination streaks around $(6, 6, 0)$, we subtracted the observed intensities at 300 K from those at 136 K. Since the thermal diffuse scattering at 300 K is larger than that at 136 K, this subtraction resulted in negative values for the difference intensity. Therefore, the calculated thermal diffuse scattering was added to the difference intensity so that the resulting distribution had positive values except for vanishing intensities along the $[1\bar{1}0]$ as predicted by calculations. From the result shown in Fig. 5, it can be seen that the butterfly-shaped pattern, as well as the small peaks around $(6 \pm \zeta, 6, 0)$ and $(6, 6 \pm \zeta, 0)$ with $\zeta = \sim 0.3$–0.35, becomes clearer. Such peaks are also seen as humps in the scattering profiles around the $(0, 10, 0)$ reflection as shown in Fig. 1. The calculations based on the assumptions of noninteracting polarons cannot explain the appearance of these peaks. They are probably attributable to the correlation between polarons. A large number of polarons should exist near T_C in the nearly half-doped system and the distortion fields should overlap with each other.

The results of the resistivity and magnetization measurements on $(Nd_{1-y}Sm_y)_{0.5}Sr_{0.5}MnO_3$ crystals suggest a subtle balance of the competition between the ferromagnetic double-exchange interaction and the antiferromagnetic charge-ordering interaction [10]. Absorption spectra of $(Nd_{1-y}Sm_y)_{0.6}Sr_{0.4}MnO_3$ above T_C are similar to those of the charge-ordered crystals [9]. In x-ray scattering studies [15] on single crystals of a typical charge-ordered system of $Pr_{1-x}Ca_xMnO_3$ ($x = 0.35$, 0.4, and 0.5) [16], similar patterns of the diffuse scattering with incommensurate peaks have been observed above the charge-ordering transition temperatures. These experimental results lead to the conclusion that the correlation between polarons is essential to the formation of the charge-ordered state.

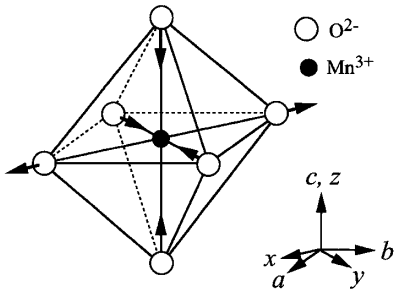

FIG. 4. The displacement pattern of a polaron associated with the Jahn-Teller effect of a $Mn^{3+}O_6$ octahedron. The arrows represent the displacements of oxygen ions.

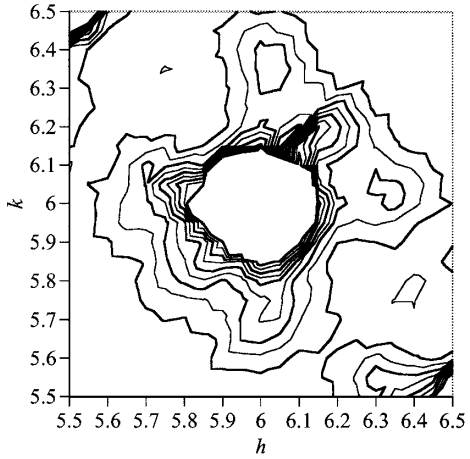

FIG. 5. Contour plot obtained by subtracting the observed intensities around $(6, 6, 0)$ at 300 K from those at 136 K. The calculated thermal diffuse scattering is added.

The details of the correlation corresponding to the wave vector near T_C are still unclear, but information about the correlation might be obtained from the charge-ordering patterns reported in various manganese oxides. Modulation wave vectors characterizing the charge-ordered state have been determined for systems with the hole concentration x larger than 0.5 [17]. In these compounds, the modulation wave vector was found to be equal to the concentration of the doped carrier, $1 - x$. The charge-ordered state may be regarded also as long-range order of polarons. Although the compound studied in the present work does not exhibit a long-range charge order, the positions of the observed diffuse peaks ($\zeta = \sim 0.3-0.35$) may be closely related to polaron concentration in this system. Recently pairs of distorted $Mn^{3+}O_6$ stripes separated by undistorted $Mn^{4+}O_6$ octahedra have been observed in the charge-ordered phases [18]. The observation may offer a clue as to the fundamental mechanism of the correlation.

It should be pointed out that the diffuse peaks can also appear if a phonon mode has a local minimum at the corresponding wave vector. This possibility cannot be eliminated and should be examined by measuring the phonon dispersion.

The authors acknowledge encouragement and support by Professor K. Tajima during the course of this study. One of the authors (N. W.) thanks Dr. S. K. Sinha for helpful discussions. This work was partly supported by a Grant-in-Aid for Science Research from the Ministry of Education, Science, Sports and Culture, Japan, and by the New Energy and Industrial Technology Development Organization (NEDO) of Japan.

*Present address: Department of Physics, Sophia University, 7-1 Kioicho, Chiyodaku, Tokyo, 102-8554 Japan, and PRESTO, JST, Japan.

[1] C. Zener, Phys. Rev. **82**, 403 (1951); P. W. Anderson and H. Hasegawa, Phys. Rev. **100**, 675 (1955); P. G. de Gennes, Phys. Rev. **118**, 141 (1960).
[2] A. J. Millis, P. B. Littlewood, and B. I. Shraiman, Phys. Rev. Lett. **74**, 5144 (1995).
[3] A. J. Millis, B. I. Shraiman, and R. Mueller, Phys. Rev. Lett. **77**, 175 (1996); H. Röder, Jun Zang, and A. R. Bishop, Phys. Rev. Lett. **76**, 1356 (1996).
[4] Guo-meng Zhao, K. Conder, H. Keller, and K. A. Müller, Nature (London) **381**, 676 (1996).
[5] C. H. Booth *et al.*, Phys. Rev. Lett. **80**, 853 (1998); T. A. Tyson *et al.*, Phys. Rev. B **53**, 13 985 (1996); A. Lanzara *et al.*, Phys. Rev. Lett. **81**, 878 (1998).
[6] Despina Louca *et al.*, Phys. Rev. B **56**, R8475 (1997); S. J. L. Billinge *et al.*, Phys. Rev. Lett. **77**, 715 (1996).
[7] K. H. Kim *et al.*, Phys. Rev. Lett. **77**, 1877 (1996).
[8] A. Machida, Y. Moritomo, and A. Nakamura, Phys. Rev. B **58**, R4281 (1998).
[9] A. Machida, Y. Moritomo, and A. Nakamura, Phys. Rev. B **58**, 12 540 (1998).
[10] H. Kuwahara *et al.*, Science **272**, 80 (1996); Y. Tokura *et al.*, Phys. Rev. Lett. **76**, 3184 (1996); H. Kuwahara *et al.*, Phys. Rev B **56**, 9386 (1997).
[11] Recently, similar diffuse scattering has been observed in $La_{1.2}Sr_{1.8}Mn_2O_7$ exhibiting the CMR phenomena; L. Vasiliu-Doloc *et al.*, Phys. Rev. Lett. **83**, 4393 (1999).
[12] N. Wakabayashi, Phys. Rev. B **17**, 3875 (1978).
[13] P. H. Dederichs, J. Phys. F **3**, 471 (1973).
[14] T. W. Darling *et al.*, Phys. Rev. B **57**, 5093 (1998).
[15] S. Shimomura *et al.* (to be published).
[16] Y. Tomioka *et al.*, Phys. Rev. B **53**, R1689 (1996).
[17] C. H. Chen, S.-W. Cheong, and Y. Hwang, J. Appl. Phys. **81**, 4326 (1997).
[18] S. Mori, C. H. Chen, and S.-W. Cheong, Nature (London) **392**, 473 (1998).